Lattice anomalies and magnetic excitations of the spin web compound Cu_3TeO_6

2008 J. Phys.: Condens. Matter 20 505214

(http://iopscience.iop.org/0953-8984/20/50/505214)

J. Phys.: Condens. Matter **20** (2008) 505214 (6pp) doi:10.1088/0953-8984/20/50/505214

Lattice anomalies and magnetic excitations of the spin web compound Cu_3TeO_6

K Y Choi[1], P Lemmens[2], E S Choi[3] and H Berger[4]

[1] Department of Physics, Chung-Ang University, 221 Huksuk-Dong, Dongjak-Gu, Seoul 156-756, Republic of Korea
[2] Institute of Condensed Matter Physics, TU Braunschweig, D-38106 Braunschweig, Germany
[3] National High Magnetic Field Laboratory, Tallahassee, FL 32306-4390, USA
[4] Institute de Physique de la Matière Complexe, EPFL, CH-1015 Lausanne, Switzerland

E-mail: kchoi@cau.ac.kr

Received 21 August 2008, in final form 21 October 2008
Published 12 November 2008
Online at stacks.iop.org/JPhysCM/20/505214

Abstract

We report on the magnetic susceptibility and Raman scattering measurements of the $S = 1/2$ three-dimensional (3D) spin web compound Cu_3TeO_6. The magnetic susceptibility shows an antiferromagnetic ordering at $T_N \sim 61$ K and a deviation from the Curie–Weiss law around 150 K. Raman spectra show the emergence of a new mode at 132 cm^{-1} for temperatures below $T^* \sim 50$ K (≈ 0.8 T_N). At the same temperature, phonon anomalies in intensity and frequency show up. This gives evidence of pronounced magneto-elastic effects. In addition, we observe a two-magnon Raman spectrum around 214 cm^{-1}. Compared to typical 3D spin systems, its robust temperature dependence suggests that a frustrated spin topology with a reduced spin coordination number also enhances spin–phonon couplings.

(Some figures in this article are in colour only in the electronic version)

1. Introduction

Since the discovery of the high-temperature superconducting cuprates, a large research effort has been devoted to investigations of magnetism based on copper oxide compounds. Cu^{2+} ions with a $3d^9$ configuration exhibit an enormous diversity of magnetic structures, depending on the effective magnetic dimensionality and frustrated magnetic interactions [1]. In particular, introducing lone-pair cations (Se^{4+} or Te^{4+}) into copper based magnetic compounds is a promising route to realize novel magnetic structures [2]. The lone-pair ions allow for an easy modification of exchange interaction paths. For instance, $Cu_2Te_2O_5X_2$ (X = Cl, Br) realizes a weakly coupled Cu_4^{2+} tetrahedra system where the spin tetrahedra are separated by lone-pair Te(IV) ions within the ab plane [3]. This system provided an unprecedented opportunity to address the interplay between localized spin singlet dynamics and collective excitations [4–6]. In contrast, $CuTe_2O_5$ realizes a spin dimer system where structural groups do not coincide with the magnetic dimers [7].

Our present study is aimed at investigating unusual magnetic properties of related systems. The title compound is a novel type of three-dimensional (3D) magnetic system Cu_3TeO_6, called a 3D spin web [8]. Cu_3TeO_6 possesses a cubic structure with space group $Ia\bar{3}$ and lattice parameters $a = 9.537$ Å [9]. The lattice consists of strongly distorted edge-sharing CuO_6 octahedra with a Cu–Cu distance of 3.18 Å (see figure 1). Six Cu^{2+} ions form an almost planar hexagon centered around a tellurium ion. There are four different orientations of hexagons, which are perpendicular to one space diagonal of the cubic unit cell. The spins are arranged in such a way that one hexagon is connected to six other hexagons by sharing one common corner. Each spin is shared by the two hexagons whose orientation belongs to a different direction of the space diagonals. From a spin topology point of view, each Cu^{2+} has four nearest neighbors and experiences a partial frustration due to a common sharing of the two non-coplanar hexagons.

The magnetic susceptibility of Cu_3TeO_6 shows antiferromagnetic (AF) correlations between copper ions and long-range magnetic ordering at $T_N = 60$ K. Neutron powder diffraction experiments evidence a collinear AF alignment of the spins within the hexagons [8]. The collinear AF ordering along the [111] direction was proposed to induce possibly a structural phase transition through a magneto-elastic

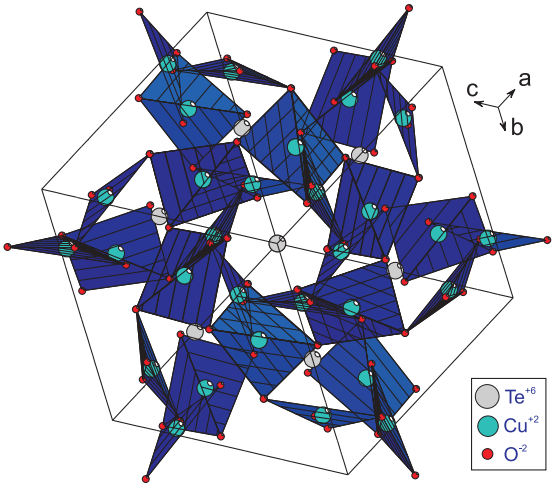

Figure 1. Sketch of the crystal structure of Cu_3TeO_6 projected along [111] [9].

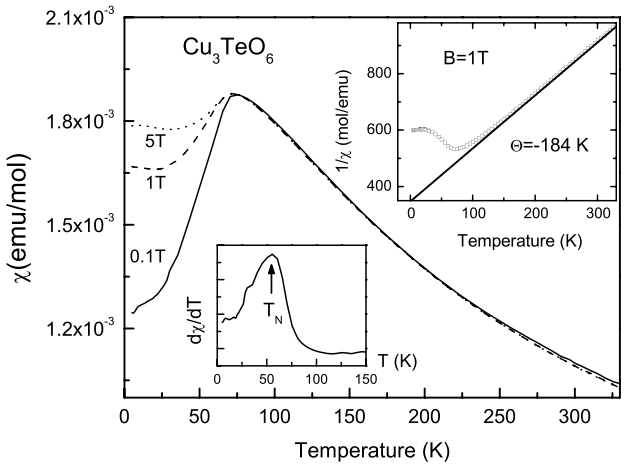

Figure 2. Temperature dependence of the static magnetic susceptibility of Cu_3TeO_6 measured at 0.1, 1, and 5 T, respectively. Upper inset: the inverse susceptibility as a function of temperature at 1 T. The solid line is a fit to the Curie–Weiss law. Lower inset: $d\chi(T)/dT$ at 1 T as a function of temperature. The jump-like anomaly indicates long-ranged magnetic ordering at $T_N = 61$ K.

strain. Remarkably, in optical reflectivity measurements the emergence of a new mode at 208 cm^{-1} has been discovered for temperatures below about $T^* = 50$ K. With decreasing temperature below T^* its intensity increases in a mean-field-like way. This was discussed in terms of a structural phase transition driven by the AF ordering [10]. However, the interrelation between the novel magnetic structure and the lattice anomalies has not yet been fully clarified. The latter also plays an important role for the observation of multiferrocity or magneto-capacitive effects in other systems with collinear order.

In this paper, we report magnetic susceptibility and Raman scattering measurements of Cu_3TeO_6. We observe salient features in low-temperature Raman spectra. The 132 cm^{-1} peak, which shows up for temperatures below $T^* = 50$ K, is identified as a phonon mode related to a structural instability. The broad maximum around 214 cm^{-1} exhibits a characteristic behavior of two-magnon scattering. Their detailed aspects are discussed in terms of spin–phonon coupling, a peculiar spin topology and spin frustration.

2. Experimental details

Single crystals of Cu_3TeO_6 were prepared by adopting the chemical transport-reaction method using $CuTeO_3$ and TeO_2 flux. Samples from the same batch have been characterized by means of neutron and magnetization measurements [8]. Magnetic susceptibility was measured by a superconducting quantum interference device (SQUID) magnetometer (MPMS, Quantum Design). Raman scattering experiments were performed using the excitation line $\lambda = 514.5$ nm of an Ar^+ laser in a quasi-backscattering geometry [11]. A comparably small laser power of 1 mW was focused to a 0.1 mm diameter spot on the surface of the single crystal in contact gas. The scattered spectra were collected on a DILOR-XY triple spectrometer and a nitrogen-cooled charge-coupled device detector.

3. Results and discussion

3.1. Magnetic susceptibility

Figure 2 displays the static magnetic susceptibility $\chi(T)$ of Cu_3TeO_6 measured at a magnetic field of $H = 0.1$, 1, and 5 T, respectively. $\chi(T)$ follows the Curie–Weiss law $\chi_{CW} = \chi_0 + C_{mol}/(T - \Theta)$ in a temperature range of 150–330 K. Here C_{mol} is the molar Curie constant and Θ is the Curie–Weiss temperature. A fit to the Curie–Weiss law is shown for $H = 1$ T in the upper inset. The fit yields $\Theta = -184$ K and an effective moment $\mu_{eff} = \sqrt{3k_B C_{mol}/N_A} = 1.86\ \mu_B$. Here k_B is the Boltzmann constant, N_A is the Avogadro number, and μ_B is the Bohr magneton. The large, negative Θ suggests that Cu^{2+} ions are antiferromagnetically coupled. The measured value of μ_{eff} is in good agreement with the theoretically estimated value of $\mu = g\mu_B\sqrt{S(S+1)} \approx 1.82\ \mu_B$ for the Cu^{2+} magnetic moment with $S = 1/2$ and a g factor $g \approx 2.1$.

For temperatures below about 150 K $\chi(T)$ starts to deviate from the Curie–Weiss behavior. At low temperature the susceptibility shows a maximum at 70 K and then a rapid drop. There is no indication for a thermal hysteresis between the field-cooled and zero-field-cooled measurements. The derivative of $\chi(T)$ with respect to temperature evidences a jump-like anomaly at $T_N = 61$ K, indicating the development of long-range ordering (see the lower inset of figure 2). This agrees well with earlier works [8, 10].

With increasing B from 0.1 to 5 T, no reduction of T_N is observed. This points to a 3D antiferromagnetic ordering with only weak spin anisotropy. The ratio of Θ to T_N, the so-called frustration index $f = \Theta/T_N = 3.0$, is moderate. This is associated with the geometrical frustration of each spin shared between the two non-coplanar hexagons. Assuming that Θ is determined by the strongest nearest-neighbor exchange coupling J yields $\Theta = -zJS(S+1)/k_B$ in the molecular-field approximation. We obtain an AF exchange interaction between

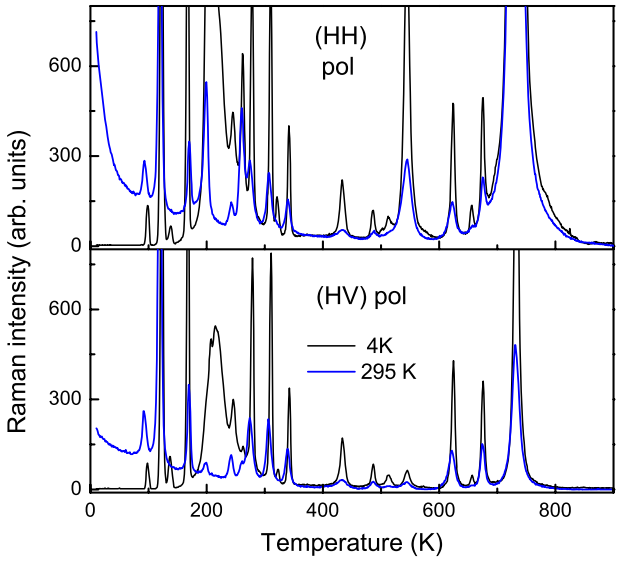

Figure 3. Raman spectra of Cu_3TeO_6 for (HH) and (HV) polarizations at $T = 4$ and 295 K, respectively.

the nearest-neighbor Cu ions of $J = 61.3$ K. Here we note that the number of nearest neighbors $z = 4$ is smaller than other 3D lattices with $z \geqslant 6$. This is because each spin is shared only by two hexagons. The exchange interaction relies on the angle and distance of Cu–O–Cu bonding [12]. In Cu_3TeO_6 the Cu–O–Cu bond angles are given by 92.4° and 106.2°. The small deviation of the bond angle from 90° explains the relatively weak antiferromagnetic exchange interaction.

3.2. Raman spectrum

Figure 3 compares Raman spectra in (HH) and (HV) polarizations at 4 and 295 K. Due to the small size of the studied sample, light is guided to a direction whose normal surface is largest, denoted by H to optimize the signal quality. Notwithstanding, it will impose no restrictions on extracting the information about the magnetic and lattice properties since Cu_3TeO_6 is networked in a three-dimensional way.

Cu_3TeO_6 has the space group $Ia3$. Subtracting the acoustic modes, the factor group analysis yields a total of 22 Raman-active modes; $4A_g(aa + bb + cc) + 4E_g(aa + bb - 2cc, \sqrt{3}aa - \sqrt{3}bb) + 14F_g(ab, ac, bc)$. For both polarizations we detect 20 peaks at room temperature as phonon scattering, which are slightly less than the theoretical prediction. By considering both the Raman matrix elements and the relative intensity of the observed phonon modes in the (HH) and (HV) polarizations, we are able to identify their symmetry; the 199, 260, 545, and 732 cm^{-1} peaks to the A_g mode, the 120, 169, 306, and 623 cm^{-1} peaks to the E_g mode, and the remaining peaks to the F_g mode. The absence of the two F_g modes has to be attributed to their small Raman scattering intensity or to degeneracies of their frequencies beyond the resolution of the present Raman scattering experiment. The high-frequency modes of 600–750 cm^{-1} correspond to the stretching modes of the Te–O bonds [13]. In the intermediate interval of 250–550 cm^{-1} several bending modes of the O–Te–O and Cu–O bonds are expected. The low-frequency modes below 250 cm^{-1} involve the coupled displacements of Cu and Te ions.

At low temperatures two distinct features appear. One is a sharp peak around 132 cm^{-1}, which emerges for temperatures below 50 K. The other is a broad maximum centered around 214 cm^{-1}. Judging from its characteristic energy scale and the temperature dependence of intensity and energy, we assign the latter to magnetic excitations. The origin of the former will be discussed below.

3.3. Lattice anomalies

In the following we will focus on the temperature dependence of the phonon frequencies and intensity. The results are extracted by fitting the corresponding spectra to Lorentzian profiles. For the phonon modes in the frequency regime 150–800 cm^{-1} we do not find any significant change in the phonon frequencies as temperature varies. Their shift is restricted to maximally 1–3 cm^{-1}, largely attributable to lattice anharmonicity (not shown here). Instead, we observe large variations of the phonon intensities. Overall, the phonons become 3–5 times more intensive with lowering the temperature from 295 to 4 K. In figure 4(a) we plot a representative example for the 623 cm^{-1} mode. Upon cooling, this phonon intensity grows monotonically while showing a kink around $T^* = 50$ K. Raman intensities are affected by intrinsic or extrinsic factors. Since the optical reflectivity shows no appreciable change as a function of temperature, the observed temperature dependence must be caused by intrinsic factors; (i) dipole matrix elements arising from a phonon-induced polarization of the wavefunction and (ii) band energies. Both factors vary substantially with ionic displacements. Thus, the strong enhancement of the phonon intensity seen below 50 K can be related to some change in ionic displacements. We note that the three-dimensionally coupled spin dimer system $TlCuCl_3$ shows a similar, drastic change of the phonon intensity, which was discussed in terms of spin–phonon coupling [14].

In magnetic systems, local binding potentials and the bulk elastic constants can be affected by the spins. Therefore the microscopic phonon frequencies are sensitive to spin correlations between nearest-neighbor pairs ($\omega \sim< S_i \cdot S_j >$) [15]. In order to identify such a magneto-elastic mechanism, we examine carefully anomalies in the phonon frequency, focusing especially on the energy scale comparable to the exchange interaction energy. Pronounced effects should be observed for such low-frequency modes whose eigenmodes modulate the complex Cu–Cu superexchange paths. Indeed, we observe a substantial hardening of the 93.5 cm^{-1} mode by 6 cm^{-1} with lowering temperature (see figure 4(b)). Moreover, a tiny softening is noticeable below $T^* = 50$ K. The anomaly is highlighted by estimating the anharmonic phonon contribution based on a phonon–phonon decay process model [16, 17]

$$\omega_{ph}(T) = \omega_0 + C\left(1 + \frac{2}{e^x - 1}\right)$$

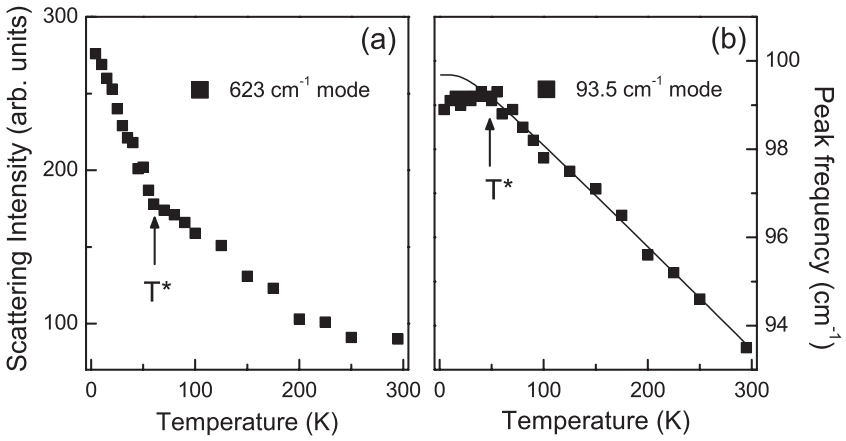

Figure 4. (a) Scattering intensity of the 623 cm^{-1} mode as a function of temperature. (b) Temperature dependence of the peak frequency of the 93.5 cm^{-1} mode. The solid line is a fit to a theoretical model. See the text for details.

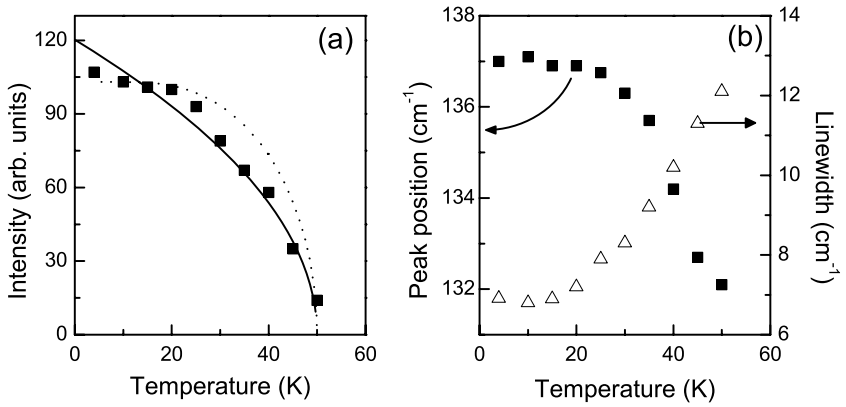

Figure 5. (a) Temperature dependence of the intensity of the 132 cm^{-1} mode. The solid line is a fit to the mean-field model and the dotted line is a Brillouin function. (b) Peak position and linewidth of the 132 cm^{-1} mode as a function of temperature.

where $x = \hbar\omega_0/2k_BT$ with the value of $\omega_0 = 100.5$ cm^{-1} and $C = -0.84$ cm^{-1}. In the paramagnetic regime, the phonon frequency increases almost linearly. This is ascribed to lattice contractions caused by lattice anharmonicities. The deviation between the fitted and experimental data starts to appear around T^*. The onset temperature of the phonon frequency anomaly coincides with the kink temperature of the phonon intensity. This supports the previous evidence for pronounced spin–phonon coupling. Compared to low-dimensional spin systems, however, the magnitude of the frequency softening is small [1, 18]. This might be due to the fact that the 3D spin web structure of the exchange paths has four different, directional preferences so that the net contribution largely averages out.

We turn now to the 132 cm^{-1} mode, which emerges for temperatures below $T^* \sim 50$ K. This mode is observed in both (HH) and (HV) polarizations. In figure 5 we summarize its intensity, peak energy, and linewidth as a function of temperature. The peak broadens and shifts to lower frequency upon heating, and it vanishes when approaching the magnetic transition temperature, T_N, from below. Based on this temperature dependence, we are likely to interpret the mode as a one-magnon excitation. A zone-center transverse magnon mode is Raman active by virtue of spin–orbit coupling and has been reported, e.g. in the spin-Peierls compound $CuGeO_3$ and the two-dimensional antiferromagnet La_2CuO_4 [19]. However, for the compound in our title this interpretation is not convincing due to its energy scale, which is even larger than the isotropic superexchange interaction J. Typically, the one-magnon mode is of the order of 10 cm^{-1} in copper oxides since the zone-center magnon gap is determined by the magnitude of anisotropic interactions.

Further information about the origin of this mode comes from optical spectroscopy experiments [10]. At the same temperature of $T^* \sim 50$ K ($\approx 0.8\ T_N$) a similar feature was observed with slightly higher energy, at 208 cm^{-1}. This energy scale, selection rule, and magnetic-field dependence rules out its magnetic origin. This together with the phonon anomalies at T^* (see figure 4) suggests that the Raman-active 132 cm^{-1} mode originates from a local lattice distortion driven by or coupled to the magnetic ordering. The preliminary dielectric constant measurements show no discernible anomaly around T^*. This makes improbable any drastic change of a lattice structure.

The temperature dependence of the intensity is compared to the square-root behavior, $(T^* - T)^{1/2}$ and the $S = 1/2$ Brillouin function, respectively. Neither perfectly describes

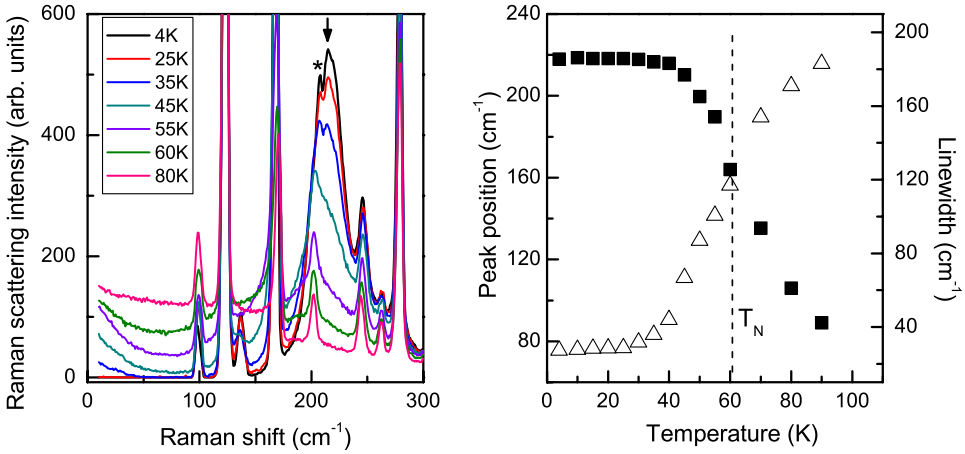

Figure 6. Left: temperature dependence of magnetic Raman spectra in (HV) polarization at 4, 25, 35, 45, 55, 60, and 80 K (from the lower to upper curve). The arrow indicates the peak position of the magnetic maximum. The asterisk indicates the phonon peak. Right: temperature dependence of the peak position (full squares, left axis) and linewidth (open triangles, right axis) of the magnetic maximum.

the temperature dependence of the intensity. The former gives a better description in the high-temperature regime while the latter fits well at low temperatures. We note that the temperature dependence of the infrared-active new mode follows the square-root dependence [10]. At present, the exact reason for the discrepancy between Raman and infrared results is not clear. In any case, we conclude that the observed temperature behavior is not simply described by the $S = 1/2$ Brillouin function. This indicates that the collinear AF system with the complex spin web structure necessitates a larger amount of magnetic energy than a low-dimensional AF one to induce a structural instability through a magneto-elastic strain.

3.4. Magnetic excitations

We now address the magnetic excitation centered around 214 cm^{-1}. In figure 6 we display the evolution of the spectral weight in (HV) polarization. Although this broad maximum overlaps with eight phonon modes, its temperature behavior can be clearly studied. With increasing temperature the magnetic continuum broadens and shifts to lower energies. At $T \gg T_N$ the maximum turns into quasi-elastic scattering. This is characteristic for two-magnon (2M) scattering originating from double spin-flip processes of an AF ground state. After subtracting the phonon modes, we determine the peak position and linewidth at half maximum. The results are summarized in the right panel of figure 6. At T_N the peak frequency is reduced by 17% and the linewidth roughly triples. For $S = 1/2$ 3D systems the magnon-pair spectral weight is typically renormalized by 25% and the damping increases by four times at T_N [20]. The robustness of the AF correlations with respect to thermal fluctuations for the title compound is attributed to the smaller coordination number than in a usual 3D lattice.

The frequency of the 2M peak of 214 cm^{-1} ($\approx$307 K) allows an estimate for the unrenormalized AF exchange constant between Cu spins. In the classical limit, the peak position lies at $J_R(2zS-1)$ where J_R is the exchange constant between neighboring Cu spins, z is the number of nearest neighboring spins, and S is the spin quantum number [20].

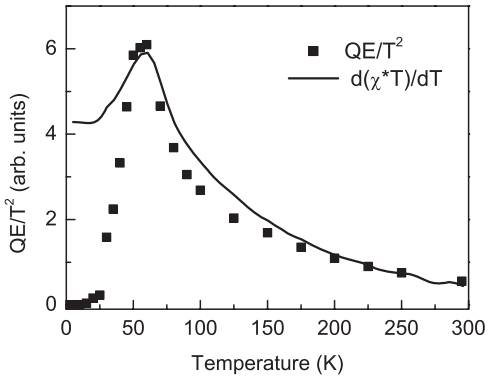

Figure 7. Temperature dependence of the integrated intensity of magnetic quasi-elastic Raman response divided by T^2 (solid square) and temperature dependence of the derivative of $\chi(T) \cdot T$ with respect to T (solid line).

For $S = 1/2$ and $z = 4$, we obtain $J_R = 102$ K. This value is roughly twice the one obtained from the molecular-field approximation (see above). This discrepancy might suggest that the actual spin topology is more complicated than the proposed 3D spin web. Alternatively, this is due to a coupling of the 2M scattering to a two phonon density of states.

Figure 7 plots the integrated intensity of magnetic quasi-elastic Raman response divided by T^2. This originates from fluctuations of the magnetic energy density of the system. This quantity is proportional to magnetic specific heat for a quantum spin system [1]. It shows the so-called Fisher's heat capacity [21], the derivative with respect to temperature of the product $\chi(T) \cdot T$. Around T_N the sharp maximum shows a λ-type anomaly with a long tail toward higher temperatures. This points to the persistence of short-range antiferromagnetic correlations to temperatures much higher than T_N, also evident from the deviation of the magnetic susceptibility from the Curie–Weiss law at the respective, higher temperatures.

4. Conclusions

In summary, we have presented magnetic susceptibility and Raman scattering measurements of the S = 1/2 3D spin web system Cu_3TeO_6. The magnetic susceptibility shows a transition to a magnetic ordering at $T_N \sim 61$ K and a deviation from the Curie–Weiss law for temperatures below 150 K. This characterizes Cu_3TeO_6 as a weakly frustrated spin system. Using Raman spectroscopy, we find a new mode at 132 cm^{-1} for temperatures well below T_N. Its intensity does not simply evolve with a $S = 1/2$ Brillouin function. The magnon energy and damping, extracted from the two-magnon spectra around 214 cm^{-1}, is more robust with respect to thermal fluctuations on the energy scale of T_N compared to conventional 3D spin systems. This suggests that in spite of a 3D spin network, spin–phonon couplings are significant due to the frustrated, complex spin topology with a reduced spin coordination number.

Acknowledgments

This work was supported by DFG and ESF-HFM.

References

[1] Lemmens P, Güntherodt G and Gros C 2003 *Phys. Rep.* **375** 1
[2] Johnsson M, Tornroos K W, Mila F and Millet P 2000 *Chem. Mater.* **12** 2853
[3] Valenti R, Saha-Dasgupta T, Gros C and Rosner H 2003 *Phys. Rev.* B **67** 245110
[4] Lemmens P, Choi K-Y, Kaul E E, Geibel C, Becker K, Brenig W, Valenti R, Gros C, Johnsson M, Millet P and Mila F 2001 *Phys. Rev. Lett.* **87** 227201
[5] Gros C, Lemmens P, Vojta M, Valenti R, Choi K-Y, Kageyama H, Hiroi Z, Mushnikov N V, Goto T, Johnsson M and Millet P 2003 *Phys. Rev.* B **67** 174405
[6] Takagi R, Johnsson M, Gnezdilov V, Kremer R K, Brenig W and Lemmens P 2006 *Phys. Rev.* B **74** 014413
[7] Deisenhofer J, Eremina R M, Pimenov A, Gavrilova T, Berger H, Johnsson M, Lemmens P, Krug von Nidda H-A, Loidl A, Lee K-S and Whangbo M-H 2006 *Phys. Rev.* B **74** 174421
[8] Herak M, Berger H, Prester M, Miljak M, Zivkovic I, Milet O, Drobac D, Popovic S and Zaharko O 2005 *J. Phys.: Condens. Matter* **17** 766
[9] Falck L, Lindquist O and Moret J 1978 *Acta Crystallogr.* B **34** 896
[10] Caimi G, Degiorgi L, Berger H and Forró L 2006 *Europhys. Lett.* **75** 496
[11] Lemmens P and Choi K Y 2005 Scattering: inelastic scattering technique—Raman *Encyclopedia of Condensed Matter Physics* ed G Bassani, G Liedl and P Wyder (Amsterdam: Elsevier)
[12] Kataev V, Choi K-Y, Grüninger M, Ammerahl U, Büchner B, Freimuth A and Revcolevschi A 2001 *Phys. Rev. Lett.* **86** 2882
[13] Nakamoto K 1986 *Infrared and Raman Spectra of Inorganic and Coordination Compounds* (New York: Wiley–Interscience)
[14] Choi K-Y, Guntherodt G, Oosawa A, Tanaka H and Lemmens P 2003 *Phys. Rev.* B **68** 174412
[15] Baltensperger W and Helman J S 1968 *Helv. Phys. Acta* **41** 668
[16] Balkanski M, Wallis R F and Haro E 1983 *Phys. Rev.* B **28** 1928
[17] Choi K-Y, Grove M, Lemmens P, Fischer M, Guntherodt G, Ammerahl U, Buchner B, Dhalenne G, Revcolevschi A and Akimitsu J 2006 *Phys. Rev.* B **73** 104428
[18] Choi K-Y, Oosawa A, Tanaka H and Lemmens P 2005 *Phys. Rev.* B **72** 024451
[19] Gozar A, Dennis B S, Blumberg G, Komiya S and Ando Y 2004 *Phys. Rev. Lett.* **93** 027001
[20] Cottam M and Lockwood D 1986 *Light Scattering in Magnetic Solids* (New York: Wiley)
[21] Fisher M E 1962 *Phil. Mag.* **17** 1731–43